

The calcium-sensing receptor is required for normal calcium homeostasis independent of parathyroid hormone

See the related Commentary beginning on page 945.

Claudine H. Kos,¹ Andrew C. Karaplis,² Ji-Bin Peng,^{1,3} Matthias A. Hediger,^{1,3} David Goltzman,⁴ Khalid S. Mohammad,⁵ Theresa A. Guise,⁵ and Martin R. Pollak¹

¹Renal Division, Department of Medicine, Brigham and Women's Hospital, Boston, Massachusetts, USA

²Division of Endocrinology, Sir Mortimer B. Davis-Jewish General Hospital, Lady Davis Institute for Medical Research, Department of Medicine, McGill University, Montreal, Quebec, Canada

³Membrane Biology Program, Brigham and Women's Hospital, Boston, Massachusetts, USA

⁴Calcium Research Laboratory, Department of Medicine, McGill University Health Centre and McGill University, Montreal, Quebec, Canada

⁵Division of Endocrinology and Metabolism, Department of Internal Medicine, University of Virginia, Charlottesville, Virginia, USA

The extracellular calcium-sensing receptor (CaR; alternate gene names, *CaR* or *Casr*) is a membrane-spanning G protein-coupled receptor. CaR is highly expressed in the parathyroid gland, and is activated by extracellular calcium (Ca^{2+}_o). Mice homozygous for null mutations in the *CaR* gene (*CaR*^{-/-}) die shortly after birth because of the effects of severe hyperparathyroidism and hypercalcemia. A wide variety of functions have been attributed to CaR. However, the lethal CaR-deficient phenotype has made it difficult to dissect the direct effect of CaR deficiency from the secondary effects of hyperparathyroidism and hypercalcemia. We therefore generated parathyroid hormone-deficient (PTH-deficient) *CaR*^{-/-} mice (*Pth*^{-/-}*CaR*^{-/-}) by intercrossing mice heterozygous for the null *CaR* allele with mice heterozygous for a null *Pth* allele. We show that genetic ablation of PTH is sufficient to rescue the lethal *CaR*^{-/-} phenotype. *Pth*^{-/-}*CaR*^{-/-} mice survive to adulthood with no obvious difference in size or appearance relative to control *Pth*^{-/-} littermates. Histologic examination of most organs did not reveal abnormalities. These *Pth*^{-/-}*CaR*^{-/-} mice exhibit a much wider range of values for serum calcium and renal excretion of calcium than we observe in control littermates, despite the absence of any circulating PTH. Thus, CaR is necessary for the fine regulation of serum calcium levels and renal calcium excretion independent of its effect on PTH secretion.

J. Clin. Invest. 111:1021-1028 (2003). doi:10.1172/JCI200317416.

Introduction

The extracellular calcium-sensing receptor (CaR) is a plasma membrane-bound G protein-coupled receptor that is activated by extracellular calcium (Ca^{2+}_o). CaR is expressed in multiple tissues including parathyroid gland, thyroid, kidney, intestine, bone, bone marrow, brain, skin, pancreas, lung, and heart (1-9). Activation of parathyroid gland CaR regulates Ca^{2+}_o .

Received for publication November 18, 2002, and accepted in revised form January 7, 2003.

Address correspondence to: Martin Pollak, Renal Division HIM 534, Brigham and Women's Hospital, Harvard Medical School, 77 Avenue Louis Pasteur, Boston, MA. 02115, USA. Phone: (617) 525-5840; Fax: (617) 525-5841; E-mail: mpollak@rics.bwh.harvard.edu.

Conflict of interest: The authors have declared that no conflict of interest exists.

Nonstandard abbreviations used: calcium-sensing receptor (CaR); extracellular calcium (Ca^{2+}_o); parathyroid hormone (PTH); familial hypocalciuric hypercalcemia (FHH); neonatal severe hyperparathyroidism (NSHPT); fractional excretion of calcium (FECa); calcium transporter type 1 (CaT1); calcium transporter type 2 (CaT2/ECaC); bone mineral density (BMD); tartrate-resistant acid phosphatase (TRAP); mineral apposition rate (MAR); bone formation rate (BFR).

homeostasis by suppressing parathyroid hormone (PTH) secretion. Mutations in the human *CASR* gene have been shown to cause familial hypocalciuric hypercalcemia (FHH), neonatal severe hyperparathyroidism (NSHPT) (10), and autosomal dominant hypocalcemia (11, 12). These Mendelian disorders are all characterized by an altered response to Ca^{2+}_o .

In 1995, Ho et al. used homologous recombination to develop a mouse model with a targeted disruption in the *CaR* gene (also known as *Casr*) in order to examine the role of CaR in calcium homeostasis and elucidate the mechanism by which inherited human *CASR* defects cause disease (13). Mice heterozygous for deficient *CaR* alleles (*CaR*^{-/-}) mimic the phenotype of patients with FHH and exhibit modest elevations in serum calcium levels with relative hypocalciuria. Mice homozygous for null *CaR* alleles (*CaR*^{-/-}) exhibit a phenotype similar to human NSHPT. *CaR*^{-/-} mice display severe hyperparathyroidism and hypercalcemia, parathyroid hyperplasia, bone abnormalities, growth retardation, and death shortly after birth (13). Most of these abnormalities are presumed to be due to the effects of hyperparathyroidism and hypercalcemia. However, both the wide tissue distribution of CaR

expression and reports of possible roles for CaR in processes not directly related to calcium homeostasis (including neuronal transmission, cellular proliferation, lymphocyte differentiation, and hormonal secretion) raise the possibility that some aspects of the phenotype in these mice (and in humans with NSPHT) may be due to an essential role for CaR signaling in these processes (14–17).

Low dietary calcium intake and hypocalcemia are major stimuli for PTH secretion leading to parathyroid gland hyperplasia (18, 19). The observed parathyroid gland hyperplasia in patients and mice with homozygous mutations in *CaR* suggests that the parathyroid gland enlargement seen during calcium deficiency may not be due to overstimulation of the gland but to a direct effect of understimulation of CaR. CaR transcripts have been identified in cartilage and bone marrow as well as in osteoclast and osteoblast cells (20–22). It has been hypothesized that local changes in Ca^{2+} , acting through CaR may serve a physiological role in regulating the differentiation and function of chondrocytes, osteoblasts, and osteoclasts and therefore may have a direct effect on bone function independent of PTH (23–25).

In order to address some of these questions, we attempted to rescue the CaR-deficient mice by genetic means. Earlier unsuccessful efforts included crossing the targeted *CaR* allele onto collagenase-resistant *Col1a1* mice (26), osteoclast-deficient *Op/Op* mice (27), and transgenic mice in which expression of wild-type CaR is targeted to the parathyroid gland (26). Here, we describe the results of our efforts to separate the direct effect of CaR deficiency from the confounding effects of hyperparathyroidism and hypercalcemia by examining the role of CaR in a mouse model that lacks PTH. Homozygous PTH-deficient mice (*Pth*^{-/-}) display diminished cartilage matrix mineralization and reduced metaphyseal osteoblasts and trabecular bone during the fetal and neonatal period, but these findings normalize in adulthood (28). We bred *CaR*^{+/-} mice with mice heterozygous for a null *Pth* allele (*Pth*^{+/-}) and crossed the double heterozygous offspring to generate mice lacking both PTH and CaR (*Pth*^{-/-}*CaR*^{-/-}). We made direct comparisons between the phenotypes of *CaR*^{-/-} mice and CaR-expressing sex-matched littermates, on *Pth*^{-/-} backgrounds, in order to assess the role of CaR independent of the effects of PTH.

Methods

Derivation of PTH and CaR double null mice. The derivation of the two parental strains of *CaR*^{-/-} mice and *Pth*^{-/-} mice by homologous recombination in embryonic stem cells was previously described by Ho et al. (13) and Miao et al. (28), respectively. Briefly, a neomycin resistance gene was inserted into exon 5 of the mouse *CaR* gene. Western blot analysis of kidney protein membrane extracts from homozygous *CaR*^{-/-} mice confirmed that no detectable protein is expressed from this allele (13). A neomycin resistance gene was inserted into exon 3 of the mouse *Pth* gene resulting in the replacement of the

entire coding sequence of mature PTH. Lack of PTH expression in parathyroid glands was confirmed by immunostaining (28). Mice heterozygous for the null *CaR* allele were previously described as being fertile (13), as were mice heterozygous for the null *Pth* allele (28). *CaR*^{+/-} mice were mated with *Pth*^{+/-} mice. Offspring heterozygous at both loci were then mated to one another in order to generate pups homozygous for both *Pth* and *CaR* null alleles (*Pth*^{-/-}*CaR*^{-/-}). Lines were maintained by breeding *Pth*^{-/-}*CaR*^{-/-} males to *Pth*^{+/-}*CaR*^{+/-} females. These mice were maintained on a mixed genetic background with contributions from C57B6, 129/SvJ, and 129/SvEv strains.

In vivo experiments. Animal protocols were approved by the institutional animal care and use committee at Harvard Medical School and were in accordance with the NIH Guide for the Care and Use of Laboratory Animals. Mice were housed in microisolator cages in a pathogen-free facility according to the regulations of the Harvard Medical School Center for Animal Resources. Water was given ad libitum. In order to prevent hypoparathyroidism-induced hypocalcemia from masking any functional effects of the null *CaR* alleles, all animals homozygous for null *Pth* alleles, regardless of *CaR* genotype, were fed a high-calcium diet (2% calcium, 0.4% phosphate, 6000 U vitamin D; Harlan Teklad-TD99224; Harlan-Teklad, Madison, Wisconsin, USA).

Genotyping of mice. Genomic DNA was isolated from tail fragments by standard phenol-chloroform extraction and isopropanol precipitation. To determine the genotype at both the *Pth* and *CaR* loci, four PCR amplification reactions were required for each animal. To assay for the presence of the wild-type *CaR* allele, samples were amplified with CaR forward primer CaR6h5' (5' TCT GTT CTC TTT AGG TCC TGA AAC A 3') and CaR reverse primer CaR6h3' (5' TCA TTG ATG AAC AGT CTT TCT CCC T 3'). To detect the presence of the null *CaR* allele, Neo forward primer r-Neo-2 (5' TCT TGA TTC CCA CTT TGT GGT TCT A 3') was used with the CaR reverse primer CaR6h3'. The wild-type *Pth* allele was detected using PTH forward primer PTHF2 (5' GAT GTC TGC AAA CAC CGT GGC TAA 3') and PTH reverse primer PTHR2 (5' TCC AAA GTT TCA TTA CAG TAG AAG 3'). The null *Pth* allele was assayed using the Neo forward primer r-Neo-2 and the PTH reverse primer PTHR2. All PCR reactions were performed using Hot Start Taq polymerase (Qiagen, Valencia, California, USA) with 35 cycles of 95°C for 17 minutes, 94°C for 30 seconds, 55°C for 30 seconds, and 72°C for 45 seconds and then a final 7-minute extension at 72°C.

Histopathology. At necropsy, mice were perfused in Bouin's fixative for several days at ambient temperature. Kidney, intestine, brain, spine, heart, lung, and bone tissues were excised and embedded in paraffin wax. The thyroid, parathyroid glands, trachea, esophagus, muscle, and adipose tissue were dissected, processed, and embedded en bloc. All sections were stained with H&E. To locate the parathyroid glands, serial sections of the thyroid bloc were cut to a thickness of 5 µm.

Analytical procedures for determining serum and urine parameters. One day before sacrifice, mice were housed in metabolic cages, and urine was collected for 16 hours overnight. Mice were sacrificed using CO₂, and blood was collected by cardiac puncture. Serum and urine calcium levels were determined using the o-cresolphthalein-complexone method (Sigma-Aldrich, St. Louis, Missouri, USA). Serum and urine creatinine levels were measured using the alkaline picrate method (Sigma-Aldrich). Serum and urine phosphorus levels were determined using the ammonium molybdate method (Sigma-Aldrich). The fractional excretion of calcium was calculated according to the following equation: $FECa = (\text{urine Ca} \times \text{plasma creatinine}) / (\text{plasma Ca} \times \text{urine creatinine}) \times 100$.

RNA isolation and preparation of cDNA. Whole kidney and duodenum were excised, frozen in liquid nitrogen and stored at -80°C until used. Tissue samples were thawed in TRIzol reagent (Invitrogen, Carlsbad, California, USA) and homogenized. RNA extraction was performed according to the TRIzol manufacturer's protocol. Reverse transcription reactions were performed using the SuperScript First-Strand Synthesis System (Invitrogen).

Detection of calcium transporter CaT1 and CaT2/ECaC expression by quantitative real-time PCR. To determine the number of cDNA molecules in the reverse-transcribed samples, real-time PCR analyses were performed using the LightCycler system (Roche Molecular Biochemicals, Indianapolis, Indiana, USA). PCR was performed using 2 µl of LightCycler DNA master SYBR Green I (Roche), 0.25 µM of each 5' and 3' primer, and 2 µl of samples or H₂O to a final volume of 20 µl. The MgCl₂ concentration was adjusted to 3 mM. Samples were denatured at 95°C for 20 seconds with a temperature transition rate of 20°C per second. Amplification and fluorescence determination were carried out in four steps: denaturation at 95°C for 0 seconds, with a temperature transition rate of 20°C per second; annealing for 5 seconds at 62°C for calcium transporter type 1 (CaT1) and calcium transporter type 2 (CaT2/ECaC) and at 60°C for GAPDH, with a temperature transition rate of 8°C per second; extension at 72°C for 20 seconds (25 seconds for GAPDH), with a temperature transition rate of 4°C per second; and detection of SYBR Green fluorescence, which reflects the amount of double-stranded DNA and was performed at 86°C (85°C for GAPDH) for 3 seconds. The amplification cycle number was 40 for CaT1 and CaT2/ECaC and 30 for GAPDH.

To discriminate specific from nonspecific cDNA products, a melting curve was obtained at the end of each run. Products were denatured at 95°C for 3 seconds, and the temperature was then decreased to 65°C for 15 seconds and raised slowly from 65°C to 95°C using a temperature transition rate of 0.1°C per second. To determine the number of copies of the targeted DNA in the samples, purified PCR fragments of known concentrations were serially diluted and served as external standards that were measured in each

experiment. Data were normalized with GAPDH levels in the samples. The primer sequences used for PCR are as follows: CaT1 forward primer, (5' ATC GAT GGC CCT GCG AAC T 3'); CaT1 reverse primer, (5' CAG AGT AGA GGC CAT CTT GTT GCT G 3'); CaT2 forward primer, (5' ATT GAC GGA CCT GCC AAT TAC AGA G 3'); CaT2 reverse primer, (5' GTG TTC AAC CCG TAA GAA CCA ACG GTC 3'); GAPDH forward primer, (5' TCA CCA TCT TCC AGG AGC G 3'); and GAPDH reverse primer, (5' CTG CTT CAC CAC CTT CTT GA 3').

Preparation of samples for bone mineral density and histomorphometric analysis. Both hind limbs were dissected out from the axial skeleton and cleared from the surrounding tissue and then immersed in 70% ethanol with the vertebral column for fixation. In addition, three pairs of mice were labeled with double fluorochromes for dynamic histomorphometric bone study. Tetracycline hydrochloride (0.03 mg/g of body weight) was administered intraperitoneally 10 days before sacrifice. Calcein (0.02 mg/g of body weight) was administered intraperitoneally 3 days before sacrifice.

Bone mineral density measurement. Bone mineral density (BMD) measurements were performed on the dissected bones using lunar PIXImus densitometry (GE Lunar Corporation, Madison, Wisconsin, USA). Measurements were conducted on the right femur and tibia, the left femur and tibia, and the lumbar spine using the image analysis software provided by the system. BMD (in

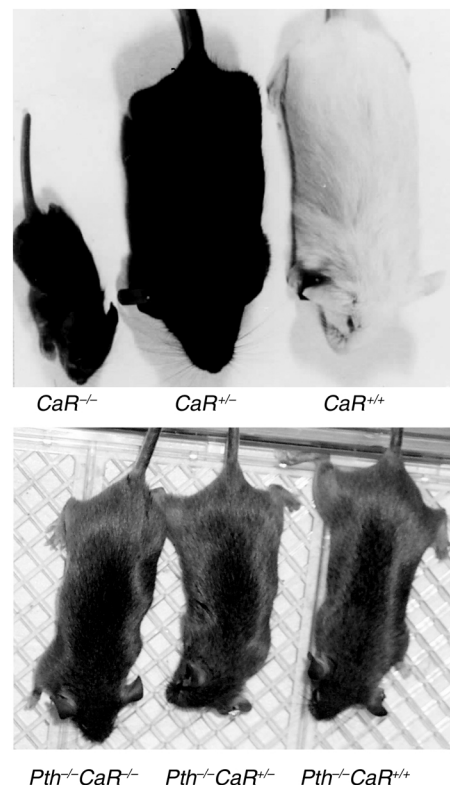


Figure 1

Gross appearance of (a) 23-day-old $CaR^{-/-}$, $CaR^{+/-}$ and $CaR^{+/+}$ mice and (b) 10-week-old $Pth^{-/-}CaR^{-/-}$, $Pth^{-/-}CaR^{+/-}$, and $Pth^{-/-}CaR^{+/+}$ mice.

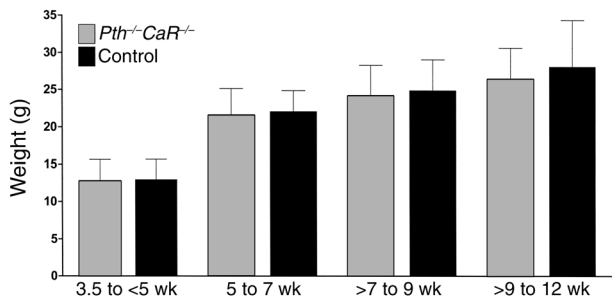


Figure 2
Body weight of *Pth*^{-/-}*CaR*^{-/-} and control mice as a function of age. *Pth*^{-/-}*CaR*^{-/-} mice (gray bars) and control sex-matched littermates (black bars) were weighed between 3.5 and 12 weeks of age. Each column represents the mean ± SD derived from 8–15 measurements.

g/cm²) was defined as the integral mass of bone mineral per unit of projected areas.

Bone histomorphometry. After fixation in 70% ethanol for 48 hours and BMD image acquisition, the undecalcified left hind limbs and the upper spine (thoracic vertebrae) were embedded in methylmetacrylate for dynamic bone studies. The right hind limbs and lower spine (lumbar and sacral regions) were decalcified, processed, and embedded in paraffin for H&E and tartrate-resistant acid phosphatase (TRAP) staining. Longitudinal mid-sagittal sections 7 μm in thickness of all the tissues were prepared for histomorphometric analysis. All measurements were performed using an Olympus microscope; images were taken and analyzed using the Metamorph software (Universal Imaging Corporation, Downingtown, Pennsylvania, USA).

Trabecular bone volume was assessed on the secondary spongiosa of the proximal tibia, distal femur, and lumbar spine at ×40 magnification on H&E-stained sections and expressed as a percentage of total tissue volume. Osteoclast number was assessed in the same regions on TRAP-stained sections at ×100 magnification and expressed as osteoclast number per millimeter of bone surface. The trabecular surface labeled with double or single labels was measured using fluorescence microscopy at ×400 magnification. Measurements were performed on two fields per section of two consecutive sections. The mineral apposition rate

(MAR) and bone formation rate (BFR) were calculated by examination of tetracycline and calcein-labeled bones as described previously (29).

Statistics. We evaluated the differences between multiple *Pth*^{-/-}*CaR*^{-/-} and control littermates using paired *t* tests. All values are expressed as means ± SD. The computations and graphs illustrated in Table 1, Figure 3, and Figure 6 were performed using the GraphPad Prism 3.0 scientific graphing, curve fitting, and statistics program for Macintosh (GraphPad Software Inc., San Diego, California, USA). In addition, we tested the data for serum calcium concentration, urine calcium/urine creatinine ratio, and fractional excretion of calcium to see if the variance of the *Pth*^{-/-}*CaR*^{-/-} animals exceeded the variance of the controls (defining the absence of a difference in the variance as the null hypothesis) using a one-sample χ^2 test (SAS/Analyst version 8, Cary, North Carolina, USA). Statistical analyses were supported in part by the Biostatistics Consulting Service of the Center for Clinical Investigation at Brigham and Women's Hospital.

Results

Rescue of lethal *CaR*-deficient phenotype in the absence of PTH. *Pth*^{-/-}*CaR*^{-/-} mice were born in predicted Mendelian ratios. The lethal phenotype of *CaR*-deficient mice previously described by Ho et al. (13) was not observed in animals also deficient for PTH. Of the over 40 animals generated that were homozygous for null alleles at both the PTH and *CaR* loci, all but two pregnant females survived well into adulthood, appeared healthy, and exhibited no visible abnormalities.

Reduced fertility of *Pth*^{-/-} mice. During attempts to establish a breeding colony, we noticed very reduced pregnancy and offspring rates in cages of *Pth*^{-/-} mice regardless of *CaR* genotype. Five *Pth*^{-/-} females died (including two *Pth*^{-/-}*CaR*^{-/-} females) during pregnancy or while lactating. We hypothesized that hypocalcemia during pregnancy and lactation was the cause of death and therefore maintained all *Pth*^{-/-} mice on a high-calcium (2%), high-vitamin D diet. To assay the affect of the high-calcium diet on serum calcium levels, two groups of *Pth*^{-/-}*CaR*^{+/+} control animals were maintained on either a regular or a high-calcium diet for 2 weeks and then sacrificed so that serum could be

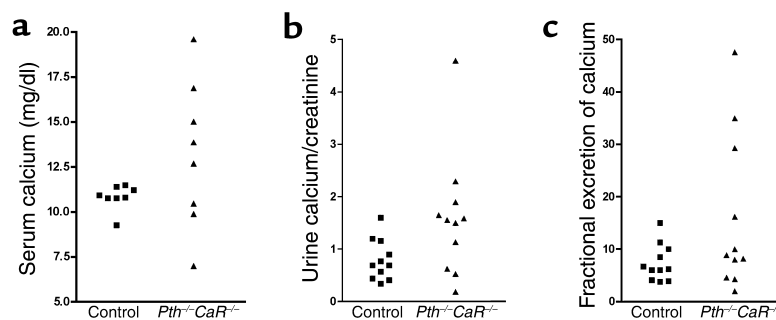


Figure 3
Graph showing the range of values for (a) serum calcium levels, (b) urine calcium to urine creatinine ratio, and (c) fractional excretion of calcium for control mice (filled squares) and *Pth*^{-/-}*CaR*^{-/-} sex-matched littermates (filled triangles).

Table 1Blood and urine profiles of *Pth*^{-/-}*CaR*^{-/-} and control mice

	Control siblings (n)	<i>Pth</i> ^{-/-} <i>CaR</i> ^{-/-} mice (n)	Mean comparison ^A	Variance comparison
Serum calcium (mg/dl)	10.8 ± 0.7 (8)	13.2 ± 4.0 (8)	NS	<i>P</i> < 0.0001 ^B
Serum phosphorus (mg/dl)	11.5 ± 3.6 (8)	12.9 ± 3.9 (8)	NS	NS
Serum creatinine (mg/dl)	0.98 ± 0.06 (8)	1.01 ± 0.05 (8)	NS	NS
Urine calcium/urine creatinine	0.79 ± 0.38 (11)	1.59 ± 1.17 (11)	NS ^C	<i>P</i> < 0.001 ^B
Fractional excretion of calcium	7.4 ± 3.5 (11)	15.8 ± 14.9 (11)	NS ^C	<i>P</i> < 0.0001 ^B
Fractional excretion of phosphorus	26.2 ± 25.9 (11)	17.1 ± 20.0 (11)	NS	NS

Results are means ± SD; *n* indicates the number of mice analyzed in paired comparisons. Fractional excretion was calculated as urine calcium (or phosphorus) × serum creatinine/urine creatinine × serum calcium (or phosphorus). NS, not significant. ^A*P* = 0.06–0.5 for two-tailed paired *t* test comparing values in *Pth*^{-/-}*CaR*^{-/-} mice and control littermates. ^B*P* < 0.001 for a one-sample χ^2 test to assess if *Pth*^{-/-}*CaR*^{-/-} variance exceeded the null hypothesis (control variance). ^CThere was a trend toward increased values for the urine calcium/urine creatinine ratio and fractional excretion of calcium in *Pth*^{-/-}*CaR*^{-/-} mice (in addition to increased variance) that did not reach statistical significance, with *P* = 0.059 and *P* = 0.082, respectively.

obtained. There was no difference in the serum calcium levels of *Pth*^{-/-}*CaR*^{+/+} mice on regular and high-calcium diets (data not shown). All animals continued to have reduced rates of reproduction, but the high-calcium diet appeared to prevent maternal death during pregnancy and nursing.

Phenotypic features of *Pth*^{-/-}*CaR*^{-/-} versus control mice. We made comparisons between *Pth*^{-/-}*CaR*^{-/-} mice and control littermates that had either the *Pth*^{-/-}*CaR*^{+/+} or *Pth*^{-/-}*CaR*^{+/-} genotype. *Pth*^{-/-}*CaR*^{-/-} mice were indistinguishable from their control littermates with respect to size, body weight, and behavior (Figures 1 and 2). We observed no differences between *CaR*-deficient mice and control littermates in light microscopic and histologic analyses of tissues from multiple organs, including gonads, thymus, brain, kidney, lung, and liver (data not shown).

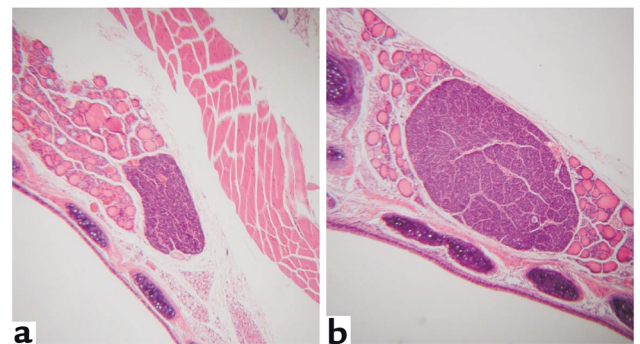
Histologic examination of parathyroid glands. Examination of the parathyroid glands from *Pth*^{-/-}*CaR*^{-/-} mice revealed a marked increase in the glandular size and hypercellularity in three out of three animals examined (Figure 3). This is consistent with earlier observations in *CaR*^{-/-} mice (14). Thus, parathyroid gland hyperplasia in *CaR*-deficient mice can occur independently of the presence of PTH. Fifty percent of the control animals (one of two *Pth*^{-/-}*CaR*^{+/-} mice and one of two *Pth*^{-/-}*CaR*^{+/+} mice) also exhibited some degree of hyperplasia.

Biochemical analyses. We measured serum and urine calcium, phosphorus, and creatinine levels (Table 1). There was a trend toward hypercalcemia and hypercalciuria in *Pth*^{-/-}*CaR*^{-/-} mice relative to controls, but the differences in these serum and urine measurements did not reach statistical significance. Further examination of the data and *P* values suggested that increasing the sample size would not increase the significance. Although the mean values for serum calcium, the urine calcium/urine creatinine ratio, and the fractional excretion of calcium were not significantly different between *Pth*^{-/-}*CaR*^{-/-} mice and control mice, the variability in these values was much greater in *Pth*^{-/-}*CaR*^{-/-} mice than in controls (Figure 3). The variation in the serum calcium levels of the *Pth*^{-/-}*CaR*^{-/-} mice (SD = 16.523) was significantly greater than the variation in controls (SD = 0.470, *P* < 0.0001) (Table 1 and Figure 4a). Similarly, the variation in the urine calcium/urine creatinine ratio of the *Pth*^{-/-}*CaR*^{-/-}

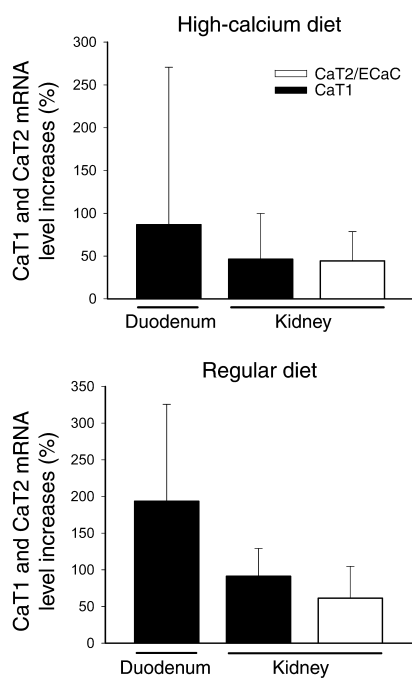
mice (SD = 1.178) was significantly greater than the variation in controls (SD = 0.3887, *P* < 0.001) (Table 1 and Figure 4b), and the variation in the fractional excretion of calcium for *Pth*^{-/-}*CaR*^{-/-} animals was significantly greater (*P* < 0.0001) than that of controls as well (Table 1 and Figure 4c).

Alterations in intestinal and renal calcium transporter expression. We assayed the mRNA expression of CaT1 (30) and CaT2/ECaC (31, 32) in the duodenum and in the kidney by quantitative real-time PCR. Results were normalized to control animal expression levels of 100%. We compared expression in RNA samples from three pairs of sex-matched littermates maintained on high-calcium diets and three pairs of sex-matched littermates on regular diets. We performed assays in duplicate for each RNA sample. CaT1 and CaT2/ECaC expression was consistently higher in the kidneys of *CaR*-deficient mice (65% and 60% higher, respectively; data from both diets) (Figure 5). These differences reached statistical significance with *P* = 0.015 and *P* = 0.0025, respectively, in paired *t* tests.

Intestinal CaT1 expression has been shown to be downregulated in animals fed high-calcium diets (33). In the mice we studied that were fed high-calcium diets, intestinal CaT1 expression was highly variable. In both the mice fed high-calcium diets and those fed regular diets, the overall trend was toward increased CaT1

**Figure 4**

Histologic appearance of parathyroid gland from control mice (a) and *Pth*^{-/-}*CaR*^{-/-} sex-matched littermates (b). Sections were prepared from adult mice for light microscopy and stained with H&E.



expression in the CaR-deficient animals, but this did not reach statistical significance either when the groups were analyzed separately according to diet or when all six pairs were analyzed together (Figure 5).

Skeletal phenotype of *Pth*^{-/-}*CaR*^{-/-} mice. We compared bones from CaR-deficient and CaR-expressing littermates (all *Pth*^{-/-}) maintained on high-calcium diets. Histologic analysis of femoral and tibial sections from *Pth*^{-/-}*CaR*^{-/-} mice revealed no apparent differences as compared with control littermates (data not shown). However, light microscopy of H&E-stained sections of vertebral bone from *Pth*^{-/-}*CaR*^{-/-} mice revealed decreased marrow space, suggesting that BMD was increased in the spines of these mice (Figure 6, b and d). Analysis of BMD measurements showed that female *Pth*^{-/-}*CaR*^{-/-} mice, but not male *Pth*^{-/-}*CaR*^{-/-} mice, have a statistically significant increase in vertebral BMD as compared with sex-matched control littermates (mean = 0.083 g/cm² and SD = 0.016 in CaR-expressing mice, mean = 0.103 g/cm² and SD = 0.24 in CaR-deficient mice, *P* = 0.043 in a one-tailed *t* test). This observation supports the hypothesis that CaR has a role in normal bone function. Measurement of osteoclast number per bone volume showed a trend toward a reduction in the number of osteoclasts in the spine per millimeter of bone volume in the *Pth*^{-/-}*CaR*^{-/-} mice but did not reach statistical significance. Measurements of BFR and MAR, performed in three pairs of littermates, did not show any consistent changes that could be attributed to CaR absence or presence.

Discussion

The Mendelian disorders of abnormal calcium homeostasis that are caused by CaR mutations are all characterized by an altered response to Ca²⁺, by the parathyroid gland and kidneys. However, CaR is

Figure 5

Expression levels of CaT1 and CaT2/EcCaC are altered in *Pth*^{-/-}*CaR*^{-/-} mice relative to control littermates. The mRNA expression levels of CaT1 (black bars) and CaT2/EcCaC (white bars) in the duodenum and kidney were assessed by real-time quantitative PCR and normalized against GAPDH mRNA levels. We compared expression in RNA samples from three pairs of sex-matched littermates maintained on high-calcium diets (2% calcium, top) and three pairs of sex-matched littermates on regular diets (0.81% calcium, bottom). We performed assays in duplicate for each RNA sample. Renal CaT1 and CaT2/EcCaC expression were consistently higher in CaR-deficient mice, regardless of diet (mean increased expression of 65% and 60%, respectively). These differences reached statistical significance with *P* = 0.015 and *P* = 0.0025, respectively, in paired *t* tests. Intestinal CaT1 expression was highly variable. In animals fed high-calcium diets as well as those fed regular diets, the overall trend was toward increased CaT1 expression in the CaR-deficient animals, but this trend did not reach statistical significance either when the groups were analyzed separately according to diet or when all six pairs were analyzed together.

expressed in multiple tissues in addition to the parathyroid glands and kidney. It has been unclear what contribution, if any, CaR mutations in these tissues make to the overall phenotypes of *CaR*^{-/-} mice and the human disorders FHH and NSHPT. Furthermore, it has been difficult to determine which abnormalities caused by inherited defects in CaR are direct effects of the CaR alterations and which are secondary to hypercalcemia and hyperparathyroidism.

In this study, we developed a CaR-deficient mouse model that survives into adulthood. By eliminating PTH, we separated the detrimental effects of hyperparathyroidism and severe hypercalcemia from the direct effects of CaR deficiency. In order to compare the effects of CaR deficiency rather than the compound effects of two mutant genes, we made all of our comparisons between *Pth*^{-/-}*CaR*^{-/-} mice and PTH-deficient

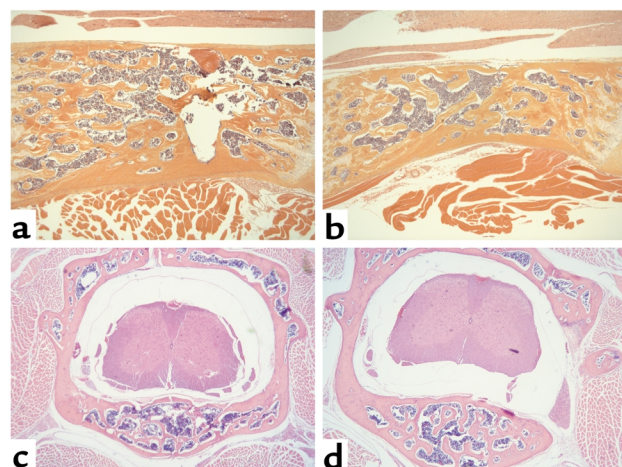


Figure 6

Morphological findings in vertebral bone of control (a and c) and *Pth*^{-/-}*CaR*^{-/-} (b and d) sex-matched littermates. Sagittal (a and b) and coronal (c and d) sections of spines from adult mice prepared for light microscopy and stained with H&E.

control sex-matched littermates (as opposed to wild-type mice). The *Pth*^{-/-}*CaR*^{-/-} mice were viable and fertile, although females had difficulty maintaining pregnancies and nursing pups when not on a calcium-enriched diet. Our results show that the major phenotypic features characteristic of *CaR*^{-/-} mice are the consequence of impaired suppression of PTH secretion and the resulting elevation in serum calcium levels and not the direct effect of CaR deficiency. This work further supports the hypothesis that the primary role of CaR is to suppress PTH secretion.

All of the *Pth*^{-/-}*CaR*^{-/-} mice had grossly enlarged parathyroid glands. Ca²⁺_o inhibits parathyroid cell proliferation. However, through studies of cyclin D1 transgenic mice, Imanishi et al. have shown that parathyroid hyperplasia can occur independently of altered Ca²⁺_o-mediated control of PTH secretion (34). Our finding that CaR-deficient mice show parathyroid hyperplasia in the absence of PTH demonstrates that parathyroid gland hyperplasia also does not depend on the overproduction of PTH per se. The enlarged parathyroid glands also observed in some of the control mice may be secondary to sustained hypocalcemia during the fetal period. Calcium is actively transported across the placenta from mother to fetus, resulting in a higher fetal calcium concentration (35–37). The parathyroid glands of a fetus in a calcium-stressed *Pth*^{-/-} mother would likely be exposed to a calcium level below normal, leading to secondary parathyroid hyperplasia.

Despite the fact that CaR-deficient mice are viable in the absence of PTH, our results indicate a role for CaR in maintaining calcium homeostasis independent of PTH. The serum calcium levels of PTH-deficient mice are much less tightly regulated in the absence of CaR. The large amount of variability between clinically significant high and low measured serum calcium values suggests that serum calcium levels in *Pth*^{-/-}*CaR*^{-/-} mice fluctuate widely. Similarly, urinary calcium excretion varied widely in mice lacking CaR. The mechanism by which CaR helps to maintain serum calcium levels within a narrow range in the absence of PTH is unclear, but this model should be useful for more detailed studies of CaR function in intestine, kidney, bone, and other homeostatic tissues. Our work indicates that CaR is necessary for the tight regulation of serum calcium levels independent of its effect on PTH secretion and that CaR is involved in fine tuning renal calcium excretion in a PTH-independent manner.

The trend in the *Pth*^{-/-}*CaR*^{-/-} animals was towards hypercalcemia and hypercalciuria. We therefore examined the expression levels of two calcium entry channels involved in the maintenance of calcium homeostasis, CaT1 (30) and CaT2/ECaC (31, 32, 38). CaT1 is expressed throughout the human gastrointestinal tract and mediates intestinal calcium absorption (30, 33, 39). CaT2/ECaC is kidney specific and localized to the apical membrane of the distal convoluted tubule (32). CaT1 and CaT2/ECaC levels in the kidney and duode-

num were increased in the *Pth*^{-/-}*CaR*^{-/-} mice, although the trend was less consistent in the duodenum than in the kidney. The increases in calcium transporter expression in the kidney and duodenum may have an impact on calcium balance and contribute to the greater variability in renal calcium excretion and serum calcium concentrations observed in the CaR-deficient mice.

We observed no detrimental bone abnormalities in *Pth*^{-/-}*CaR*^{-/-} mice. However, our measurements found that female *Pth*^{-/-}*CaR*^{-/-} mice have elevated BMD in the spine. Since multiple hypotheses were tested in the course of the various studies described in this paper, we acknowledge the possibility that this result may represent a “false positive,” particularly given the *P* value of 0.043, which is just under the generally accepted value of 0.05. However, this finding is consistent with complementary findings from other studies. Genetic factors have been shown to account for about 50–85% of the variation in bone mass, and *CaR* has been examined as a possible susceptibility locus for osteoporosis. An A986S *CaR* polymorphism has been reported to have an effect on serum calcium, circulating PTH concentrations, and BMD in healthy Caucasian girls (40, 41). (A second group found no significant difference in the distribution of the A986S polymorphism between groups of postmenopausal and healthy control women and concluded that CaR had no effect on BMD [42]). Other investigators have shown that high Ca²⁺_o stimulates CaR in chondrogenic cell lines, leading to increased production of mineral matrix (43).

We have demonstrated that the lethal CaR-deficient phenotype is dependent on PTH. In the absence of PTH, serum calcium levels and urine calcium excretion are much less tightly regulated in CaR-deficient mice than in mice with CaR. These mice provide a model for more detailed examination of the role of CaR in a wide variety of physiological functions that cannot be addressed by studying mice deficient only in CaR. These findings also have implications for understanding the role of CaR in regulating bone function independently of its effect on PTH secretion.

Acknowledgments

This work was supported by grants F32 DK09937 (to C.H. Kos), DK 52479 (to M.R. Pollak), and DK 48330 (to T.A. Guise) from the NIH/National Institute of Diabetes, Digestive, and Kidney Diseases as well as by grants from the MRC/Canadian Institutes for Health Research (to A.C. Karaplis and to D. Goltzman) and the Burroughs-Wellcome fund (to M.R. Pollak).

1. Malaisse, W.J., et al. 1999. Possible participation of an islet B-cell calcium sensing receptor in insulin release. *Endocrine*. **11**:293–300.
2. Rutten, M.J., et al. 1999. Identification of a functional Ca²⁺-sensing receptor in normal human gastric mucous epithelial cells. *Am. J. Physiol.* **277**:G662–G670.
3. Riccardi, D., et al. 1996. Localization of the extracellular Ca²⁺-sensing receptor and PTH/PTHrP receptor in rat. *Am. J. Physiol.* **271**:F951–F956.
4. Ruat, M., Molliver, M., Snowman, A., and Snyder, S. 1995. Calcium sensing receptor: molecular cloning in rat and localization to nerve terminals. *Proc. Natl. Acad. Sci. U. S. A.* **92**:3161–3165.
5. Garrett, J.E., et al. 1995. Calcitonin-secreting cells of the thyroid express an extracellular calcium receptor gene. *Endocrinology*. **136**:5202–5211.

6. Bikle, D.D., Ratnam, A., Mauro, T., Harris, J., and Pillai, S. 1996. Changes in calcium responsiveness and handling during keratinocyte differentiation. Potential role of the calcium receptor. *J. Clin. Invest.* **97**:1085–1093.
7. House, M.G., et al. 1997. Expression of an extracellular calcium-sensing receptor in human and mouse bone marrow cells. *J. Bone Miner. Res.* **12**:1959–1970.
8. Aida, K., Koishi, S., Tawata, M., and Onaya, T. 1995. Molecular cloning of a putative Ca(2+)-sensing receptor cDNA from human kidney. *Biochem. Biophys. Res. Commun.* **214**:524–529.
9. Tu, C.L., Oda, Y., and Bilke, D.D. 1999. Effects of a calcium receptor activator on the cellular response to calcium in human keratinocytes. *J. Invest. Dermatol.* **113**:340–345.
10. Pollak, M.R., et al. 1993. Mutations in the human Ca(2+)-sensing receptor gene cause familial hypocalciuric hypercalcemia and neonatal severe hyperparathyroidism. *Cell.* **75**:1297–1303.
11. Pollak, M., et al. 1994. Autosomal dominant hypocalcaemia caused by Ca2+-sensing receptor gene mutation. *Nat. Genet.* **8**:303–307.
12. Pearce, S.H., et al. 1996. A familial syndrome of hypocalcemia with hypercalciuria due to mutations in the calcium-sensing receptor. *N. Engl. J. Med.* **335**:1115–1122.
13. Ho, C., et al. 1995. A mouse model of human familial hypocalciuric hypercalcemia and neonatal severe hyperparathyroidism. *Nat. Genet.* **11**:389–394.
14. Bruce, J.I., et al. 1999. Molecular and functional identification of a Ca2+ (polyvalent cation)-sensing receptor in rat pancreas. *J. Biol. Chem.* **274**:20561–20568.
15. Cheng, I., et al. 1999. Expression of an extracellular calcium-sensing receptor in rat stomach. *Gastroenterology.* **116**:118–126.
16. Chattopadhyay, N., et al. 1997. Calcium-sensing receptor in the rat hippocampus: a developmental study. *Brain Res. Dev. Brain Res.* **100**:13–21.
17. Hennings, H., et al. 1980. Calcium regulation of growth and differentiation of mouse epidermal cells in culture. *Cell.* **19**:245–254.
18. Chen, H., et al. 2001. Effect of low calcium diet on the ultrastructure of the rat parathyroid gland. *Okajimas Folia Anat. Jpn.* **78**:153–159.
19. Brandi, M.L. 1997. Molecular mechanisms of parathyroid hyperplasia and neoplasia. *Horm. Res.* **47**:194–198.
20. Kanatani, M., Sugimoto, T., Kanzawa, M., Yano, S., and Chihara, K. 1999. High extracellular calcium inhibits osteoclast-like cell formation by directly acting on the calcium-sensing receptor existing in osteoclast precursor cells. *Biochem. Biophys. Res. Commun.* **261**:144–148.
21. Kameda, T., et al. 1998. Calcium-sensing receptor in mature osteoclasts, which are bone resorbing cells. *Biochem. Biophys. Res. Commun.* **245**:419–422.
22. Garner, S.C., Pi, M., Tu, Q., and Quarles, L.D. 2001. Rickets in cation-sensing receptor-deficient mice: an unexpected skeletal phenotype. *Endocrinology.* **142**:3996–4005.
23. Wang, D., et al. 2001. Alterations in the sensing and transport of phosphate and calcium by differentiating chondrocytes. *J. Biol. Chem.* **276**:33995–34005.
24. Yamaguchi, T., et al. 2000. Enhanced expression of extracellular calcium sensing receptor in monocyte-differentiated versus undifferentiated HL-60 cells: potential role in regulation of a nonselective cation channel. *Calcif. Tissue Int.* **66**:375–382.
25. Lorget, F., et al. 2000. High extracellular calcium concentrations directly stimulate osteoclast apoptosis. *Biochem. Biophys. Res. Commun.* **268**:899–903.
26. Zhao, W., Byrne, M.H., Boyce, B.F., and Krane, S.M. 1999. Bone resorption induced by parathyroid hormone is strikingly diminished in collagenase-resistant mutant mice. *J. Clin. Invest.* **103**:517–524.
27. Marks, S.C.J., and Lane, P.W. 1976. Osteopetrosis, a new recessive skeletal mutation on chromosome 12 of the mouse. *J. Hered.* **67**:11–18.
28. Miao, D., He, B., Karaplis, A.C., and Goltzman, D. 2002. Parathyroid hormone is essential for normal fetal bone formation. *J. Clin. Invest.* **109**:1173–1182. doi:10.1172/JCI200214817.
29. Uy, H.L., et al. 1997. Tumor necrosis factor enhances parathyroid hormone-related protein-induced hypercalcemia and bone resorption without inhibiting bone formation in vivo. *Cancer Res.* **57**:3194–3199.
30. Peng, J.B., et al. 1999. Molecular cloning and characterization of a channel-like transporter mediating intestinal calcium absorption. *J. Biol. Chem.* **274**:22739–22746.
31. Hoenderop, J.G., et al. 1999. Molecular identification of the apical Ca2+ channel in 1,25-dihydroxyvitamin D3-responsive epithelia. *J. Biol. Chem.* **274**:8375–8378.
32. Peng, J.B., et al. 2000. A rat kidney-specific calcium transporter in the distal nephron. *J. Biol. Chem.* **275**:28186–28194.
33. Van Cromphaut, S.J., et al. 2001. Duodenal calcium absorption in vitamin D receptor-knockout mice: functional and molecular aspects. *Proc. Natl. Acad. Sci. U. S. A.* **98**:13324–13329.
34. Imanishi, Y., et al. 2001. Primary hyperparathyroidism caused by parathyroid-targeted overexpression of cyclin D1 in transgenic mice. *J. Clin. Invest.* **107**:1093–1102.
35. Kovacs, C.S., et al. 1998. Regulation of murine fetal-placental calcium metabolism by the calcium-sensing receptor. *J. Clin. Invest.* **101**:2812–2820.
36. Kovacs, C.S. 2001. Calcium and bone metabolism in pregnancy and lactation. *J. Clin. Endocrinol. Metab.* **86**:2344–2348.
37. Marx, S., Fraser, D., and Rapaport, A. 1985. Familial hypocalciuric hypercalcemia. Mild expression of the gene in heterozygotes and severe expression in homozygotes. *Am. J. Med.* **78**:15–22.
38. Peng, J.B., and Hediger, M.A. 2002. A family of calcium-permeable channels in the kidney: distinct roles in renal calcium handling. *Curr. Opin. Nephrol. Hypertens.* **11**:555–561.
39. Wood, R.J., Tchack, L., and Taparia, S. 2001. 1,25-Dihydroxyvitamin D3 increases the expression of the CaT1 epithelial calcium channel in the Caco-2 human intestinal cell line. *BMC Physiol.* **1**:11.
40. Lorentzon, M., Lorentzon, R., Lerner, U.H., and Nordstrom, P. 2001. Calcium sensing receptor gene polymorphism, circulating calcium concentrations and bone mineral density in healthy adolescent girls. *Eur. J. Endocrinol.* **144**:257–261.
41. Eckstein, M., et al. 2002. Vitamin D and calcium-sensing receptor genotypes in men and premenopausal women with low bone mineral density. *Isr. Med. Assoc. J.* **4**:340–344.
42. Takacs, I., et al. 2002. Lack of association between calcium-sensing receptor gene “A986S” polymorphism and bone mineral density in Hungarian postmenopausal women. *Bone.* **30**:849–852.
43. Chang, W., Tu, C., Pratt, S., Chen, T.H., and Shoback, D. 2002. Extracellular Ca(2+)-sensing receptors modulate matrix production and mineralization in chondrogenic RCJ3.1C5.18 cells. *Endocrinology.* **143**:1467–1474.